

Seismic response and damage development analyses of an RC structural wall building using macro-element

Miloud Hemsas^{*1}, Sidi-Mohammed Elachachi^{2a} and Denys Breysse^{2b}

¹LSTE, Department of Sciences and Techniques (Civil Engineering), University of Mascara, BP 763, Route de Mamounia, 29000, Mascara, Algérie

²I2M-GCE, CNRS, UMR5295, Department of Civil and Environmental Engineering, University of Bordeaux 1, Bat. B 18, Av des Facultés, 33405 Talence, France

(Received January 26, 2013, Revised May 5, 2014, Accepted May 9, 2014)

Abstract. Numerical simulation of the non-linear behavior of (RC) structural walls subjected to severe earthquake ground motions requires a reliable modeling approach that includes important material characteristics and behavioral response features. The objective of this paper is to optimize a simplified method for the assessment of the seismic response and damage development analyses of an RC structural wall building using macro-element model. The first stage of this study investigates effectiveness and ability of the macro-element model in predicting the flexural nonlinear response of the specimen based on previous experimental test results conducted in UCLA. The sensitivity of the predicted wall responses to changes in model parameters is also assessed. The macro-element model is next used to examine the dynamic behavior of the structural wall building—all the way from elastic behavior to global instability, by applying an approximate Incremental Dynamic Analysis (IDA), based on Uncoupled Modal Response History Analysis (UMRHA), setting up nonlinear single degree of freedom systems. Finally, the identification of the global stiffness decrease as a function of a damage variable is carried out by means of this simplified methodology. Responses are compared at various locations on the structural wall by conducting static and dynamic pushover analyses for accurate estimation of seismic performance of the structure using macro-element model. Results obtained with the numerical model for rectangular wall cross sections compare favorably with experimental responses for flexural capacity, stiffness, and deformability. Overall, the model is qualified for safety assessment and design of earthquake resistant structures with structural walls.

Keywords: RC structural walls; macro-element; pushover analysis; incremental dynamic analysis; equivalent SDOF system; damage index; seismic performance

1. Introduction

Reinforced concrete (RC) structural walls are effective for resisting lateral loads imposed by wind or earthquakes on building structures. The walls can provide substantial lateral strength and stiffness to limit damage in other structural components during earthquake ground motions;

*Corresponding author, Associate Professor, E-mail: mm_hemsas@yahoo.fr

^aAssociate Professor, E-mail: sm.elachachi@i2m.u-bordeaux1.fr

^bProfessor, E-mail: d.breysse@i2m.u-bordeaux1.fr

therefore, inelastic deformations are expected, usually at the base of the wall. Significant efforts have been made recently to develop improved design provisions for calculating the strength, lateral stiffness and reinforcement details of concrete structural walls (Paulay and Priestley 1992, Wallace 1994, 1995). The nonlinear behavior of such structural systems under seismic loading should be accurately described by a reliable modeling approach that incorporate important material characteristics and behavioral response features such as neutral axis migration, concrete tension-stiffening, nonlinear shear behavior, and the effect of fluctuating axial force on strength, stiffness, and inelastic deformation capacity. For these models to be verified, experimental research is continuously conducted on RC structural walls tested under monotonic, cyclic, and dynamic loading (Vulcano and Bertero 1988, Thomsen and Wallace 1995, Lestuzzi and Bachmann 2007).

The numerical modeling of RC walls is not only involved in the applications for new construction, but it is also extended to the applications of retrofitting of existing structures. In that case, it is important to construct a representative model that is able to predict response of an existing RC structural wall under a given lateral load hazard, and to predict its expected mode of failure in order to be able to choose the most suitable and effective retrofitting technique to reach a target performance.

Nonlinear analysis of a structural wall includes two types of models: microscopic model and macroscopic model. Microscopic models such as the finite element analysis or fiber analysis are based on a detailed description of the local behavior of different materials that compose the RC element and their interaction (Miao *et al.* 2006, Belmouden and Lestuzzi 2007). Although microscopic models can provide a refined and detailed definition of the local response, this approach is complex in interpreting the results and needs high numerical processing efforts, and hence it might not be practical for large structures and it is limited to model individual structural components such as a column, or a beam. Macroscopic models, on the other hand, are based on representing the overall behavior of the RC element, such as the wall deformations, strength, and energy dissipation capacity (Kabeyasawa *et al.* 1983, Wallace 1994, 1995). The global behavior of the RC element using a macroscopic model should be calibrated thanks to an experimental verification. This approach is practical, efficient and does not require high numerical efforts, however its application is restricted based on its simplifying assumptions (Vulcano and Bertero 1987).

An effective model for analysis and design of most systems should be relatively simple to implement and reasonably accurate in predicting the nonlinear response of RC wall systems. As discussed by Vulcano and Bertero (1987), the nonlinear analysis of RC wall systems can be efficiently carried out by using analytical and numerical models based on a macroscopic approach rather than by using detailed microscopic models. Various analytical models, such as Equivalent Beam-Column Model, Equivalent Truss Model and Fiber Model, are developed to simplify structural wall element in nonlinear seismic response analysis of RC structural walls.

Although beam-column element models with rigid plastic hinges at the member ends are relatively easy to use, and are computationally efficient (stiffness parameters and plastic hinge rotation limits are easily assigned), the main limitation of a beam-column model lies in the assumption that rotations occur about the centroidal axis of the wall. Thus, important features of the observed behavior associated with variation of the neutral axis along the wall cross section, rocking of the wall, and influence of variation in axial load on the wall strength and stiffness, are disregarded and the resulting effects on the structural system are not properly considered (Kabeyasawa *et al.* 1983).

Various macroscopic models have been proposed in order to capture important behavioral

attributes for predicting the inelastic response of RC structural walls. The macro-model proposed by Vulcano *et al.* (1988) has been shown to successfully balance the simplicity of a macroscopic model and the refinements of a microscopic model. Although extensive research has been carried out with more recent modifications for the description and development of the model (Fajfar and Fischinger 1988, Fischinger *et al.* 1991, 1992), the physical phenomena underlying the response of the model to quasi-static and dynamic loading have not been rigorously studied; the model has not been sufficiently verified against extensive experimental data for both global and local responses, and important modeling parameters have not been clearly identified to obtain the nonlinear dynamic response of the model. The model also has not been implemented into widely available computer programs and limited information is available on the influence of material behavior on predicted responses.

Given these shortcomings, the goal of this paper is to investigate seismic response and damage development analyses for RC wall systems using macro-element model, as well as to validate it against experimental data including nonlinear dynamic responses, via adaptation of an approximate incremental dynamic analysis algorithm to predict seismic performance of the model and provide information about potential damage of the structural wall under damaging earthquakes.

In that respect, the effectiveness of the macro-element for modeling and simulating the inelastic response of reinforced concrete structural walls is demonstrated first. The accuracy of the model is then assessed by comparing numerically simulated responses to those obtained from experimental studies of structural walls with rectangular cross sections. Appropriate nonlinear analysis strategies were adopted in order to compare model results with results of the drift-controlled tests subjected to prescribed lateral displacement histories. The correlation of the experimental and analytical results is investigated at various response levels and locations (forces, displacements, and strains in the wall model).

The macro-element model is next used to examine the dynamic behavior of the structural wall building. Several methodologies have been proposed, the most promising one is Incremental Dynamic Analysis (IDA) procedure or dynamic pushover analysis (Vamvatsikos and Cornell 2002, Vamvatsikos and Fragiadakis 2010). It takes the basic concept of scaling ground motion record and develops it into a way to accurately describe the full range of structural behavior, from elasticity to collapse. Specifically, IDA involves subjecting a structural model to one (or more) ground motion record(s), each scaled to multiple levels. The result is a curve that shows the response of the structural model in terms of Damage Measure (*DM*) plotted against the Intensity Measure (*IM*) used to control the increment of the ground motion.

The formulation of the analytical model, the constitutive material models used in this study and approximate IDA procedure including simulation of collapse process of structural-wall elements were implemented into a finite element (FE) structural analysis code using Matlab (Math-Works 2007). The following section describes attributes of the model response and analysis of predicted numerical results at specific locations of the model parameters.

2. Macro-element model

A brief description of the wall model is presented in this section. The structural wall is discretized into a stack of (*N*) macro-elements (Fig. 1(b)), each macro-element corresponding to a level of the structure. The flexural response is simulated by a series of (*n*) uniaxial sub-elements

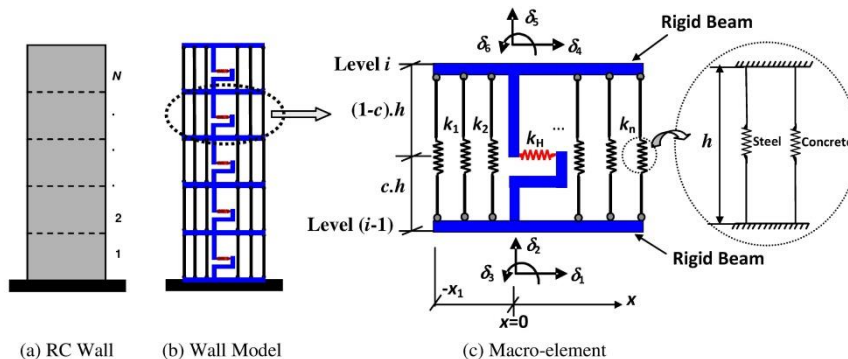


Fig. 1 Model presentation of the RC structural wall

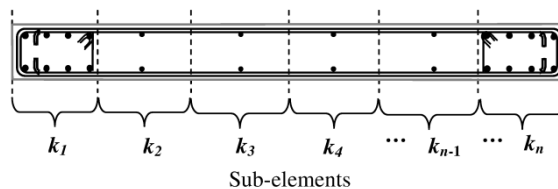


Fig. 2 Tributary area assigned to each sub-element

connected to infinitely rigid beams at the top and bottom floor: the two external sub-elements (with stiffnesses k_1 and k_n) represent the axial stiffnesses of the boundary elements, while the other elements (with stiffnesses k_2, \dots, k_{n-1}) represent the axial stiffness of the central panel (Fig. 1(c)). A given macro-element has six global degrees of freedom, two sets of three DOFs respectively corresponding to the rigid top and bottom beams. The main simplifying assumption is that these two beams remain rigid.

The only parameters associated with the analytical wall model are the total number N of macro-elements along the height of the wall, the number n of uniaxial sub-elements used across the wall cross-section, and the parameter c defining the location of the center of rotation along the height of each macro-element.

The stiffness properties and force-displacement relationships of uniaxial sub-elements are defined according to constitutive stress-strain relationships implemented for concrete and steel constitutive models and the tributary area assigned to each uniaxial sub-element (Fig. 2). The strains in concrete and steel are typically assumed to be equal (perfect bond) within each uniaxial sub-element (Fig. 1(c)). The number of the uniaxial sub-elements (n) can be increased to obtain a more refined description of the wall cross section.

The shear response of the wall element is simulated thanks to the horizontal spring with stiffness K_H , possibly with a nonlinear hysteretic force-deformation relationship. Since this study focuses on modeling of the flexural response; a linear elastic force-deformation behavior was adopted for the horizontal “shear” spring. The relative rotation of a wall member was intended around the point placed on the central axis at elevation ch , assuming a suitable value for c on the basis of the expected curvature distribution along the inter-story height h . Calculation with different values of c ($0 \leq c \leq 1$) was carried out by Vulcano *et al.* (1988) and the best result was

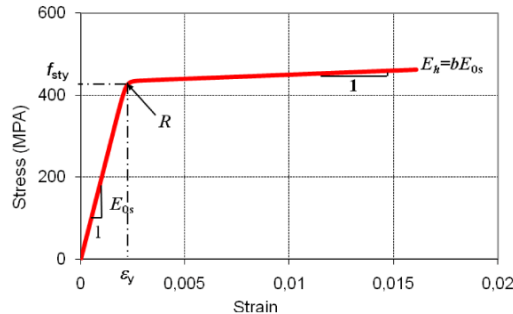


Fig. 3 Constitutive model for reinforcing steel (after Menegotto and Pinto 1973)

obtained when $c=0.4$, which was taken in this paper. According to Fischinger *et al.* (1992) an accurate assessment of c is not necessary if a moderate number of macro-elements are used within the yielding region where inelastic deformations are expected.

3. Constitutive models of steel and concrete

3.1 Steel Stress–Strain relationship

Models for steel bars stress-strain relationship which explicitly include nonlinear behavior have been developed by several researchers (Menegotto and Pinto 1973, Mander *et al.* 1988, Belarbi and Hsu 1994). The reinforcing steel stress-strain behavior implemented in the wall model is shown in Fig. 3, and is described by the nonlinear Menegotto-Pinto model (Menegotto and Pinto 1973) with a modification to include isotropic strain hardening (Filippou *et al.* 1992, Elmorsi *et al.* 1998). The model is computationally efficient and capable to reproduce experimental results with accuracy while using few physically meaningful parameters. The relationship corresponds to a curved transition (Fig. 3) from a straight-line with slope E_{0s} (modulus of elasticity) to an asymptote with slope $E_h=bE_{0s}$ (yield modulus) where the parameter b is the strain-hardening ratio. The transition curve between the two lines is governed by a curvature parameter R , experimentally calibrated by prior researchers ($R=20$, by Menegotto and Pinto (1973), Elmorsi *et al.* (1998)) based on results of cyclic tests on reinforcing bars.

3.2 Concrete Stress-Strain relation

Since concrete is used mostly in compression, the stress–strain relationship in compression is of primary importance. Many studies have been conducted on the mechanical stress-strain relationship of concrete confined by transverse reinforcement under compression. Observations and laboratory tests have shown that if the compression zone of a concrete component is confined by closely-spaced stirrup ties, hoops or spirals, the ductility of concrete is significantly enhanced and the member can sustain large inelastic deformations (Kent and Park 1971). The modified Kent-Scott-Park concrete model (Scott *et al.* 1982) is adopted, as shown in Fig. 4, to describe the strength and ductility of concrete in confined area. Even though more accurate and complete

monotonic stress-strain models have been published since, the so-called modified Kent-Scott-Park model offers a good balance between simplicity and accuracy, and is widely used. The monotonic envelope curve for concrete in compression is described by three regions. Adopting the convention that compression is positive, the three regions are

$$\text{OA Branch:} \quad \varepsilon_c \leq \varepsilon_0 \quad \sigma_c = Kf'_c \left[2 \left(\frac{\varepsilon_c}{\varepsilon_0} \right) - \left(\frac{\varepsilon_c}{\varepsilon_0} \right)^2 \right] \quad (1)$$

$$\text{AB Branch:} \quad \varepsilon_0 \leq \varepsilon_c \leq \varepsilon_{20} \quad \sigma_c = Kf'_c [1 - Z(\varepsilon_c - \varepsilon_0)] \quad (2)$$

$$\text{BC Branch:} \quad \varepsilon_c > \varepsilon_{20} \quad \sigma_c = 0.2Kf'_c \quad (3)$$

The corresponding tangent modulus E_t is given by the following expressions

$$\varepsilon_c \leq \varepsilon_0 \quad E_t = \left[\left(\frac{2Kf'_c}{\varepsilon_0} \right) \left(1 - \frac{\varepsilon_c}{\varepsilon_0} \right) \right] \quad (4)$$

$$\varepsilon_0 \leq \varepsilon_c \leq \varepsilon_{20} \quad E_t = -ZKf'_c \quad (5)$$

$$\varepsilon_c > \varepsilon_{20} \quad E_t = 0 \quad (6)$$

where

$$\varepsilon_0 = 0.002K \quad (7)$$

$$K = 1 + \frac{\rho_s f_{yh}}{f'_c} \quad (8)$$

$$\varepsilon_u = \varepsilon_0 + 0.8/Z \quad (9)$$

$$Z = \frac{0.5}{\frac{3 + 0.29f'_c}{145f'_c - 1000} + 0.75\rho_s \sqrt{\frac{h'}{s_h}} - 0.002K} \quad (10)$$

In Eqs. (1)-(10), ε_0 is the concrete strain at maximum compressive stress, ε_{20} is the concrete strain at 20% of maximum compressive stress, K is a factor that accounts for the strength increase due to confinement (for unconfined concrete, the parameter K is equal to unity), Z is the strain softening slope, f'_c is the concrete compressive strength (unconfined peak compressive stress) in MPa, f_{yh} is the yield strength of transverse reinforcement in MPa, ρ_s is the ratio between the confined volume and the total volume, h' is the width of concrete core measured to the outside of the hoops or ties, and s_h is the center to center spacing of tie or hoop sets.

In tension, the stress-strain relationship proposed by Belarbi and Hsu (1994) takes the form (Fig. 4)

$$\text{If } \varepsilon_c \leq \varepsilon_{cr} \quad \text{then} \quad \sigma_c = E_c \varepsilon_c \quad (11)$$

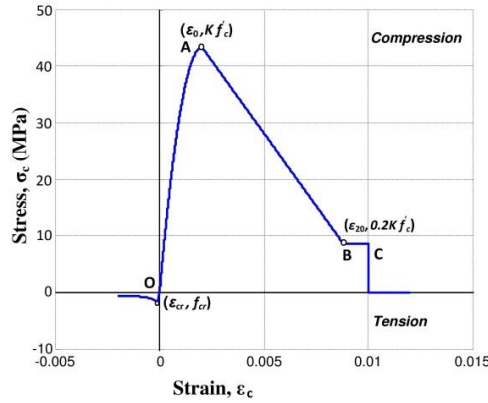


Fig. 4 Modified Kent-Scott-Park model for concrete

$$\text{If } \varepsilon_c > \varepsilon_{cr} \quad \text{then} \quad \sigma_c = f_{cr} \left(\frac{\varepsilon_{cr}}{\varepsilon_c} \right)^{0.4} \tag{12}$$

where

$$E_c = 3875 \sqrt{f_c'} \text{ (MPa)} \tag{13}$$

$$f_{cr} = 0.31 \sqrt{f_c'} \text{ (MPa)} \tag{14}$$

$$\varepsilon_{cr} = 8.10^{-5} \tag{15}$$

where, ε_c is the average concrete tensile strain, σ_c is the average concrete tensile stress, E_c is the initial Young’s modulus of the average stress-strain relation, f_{cr} is the concrete cracking stress, and ε_{cr} is the concrete strain at cracking. The expressions for f_{cr} , ε_{cr} , E_c , and the power constant 0.4 in Eq. (12) are obtained from the average and best fit of experimental results from testing of 17 RC panels with concrete compressive strengths ranging between 36.9 MPa and 47.7 MPa.

The contribution of tensile concrete resistance between cracks which is known as the tension stiffening phenomenon plays a significant role in reducing the post-cracking deformations of reinforced concrete structures. It has been recognized by different researchers (Belarbi and Hsu 1994, Pang and Hsu 1995, Mansour *et al.* 2001, Hsu and Zhu 2002) to considerably influence the post-cracking stiffness, yield capacity, and shear behavior of reinforced concrete members.

Based on extensive tests of reinforced concrete panels subjected to normal stresses, the tension-stiffening models proposed by Belarbi and Hsu (1994) have been used and validated experimentally in more recent studies to model the shear behavior of RC membrane elements (Mansour *et al.* 2001, Hsu and Zhu 2002, Bakir and Boduroglu 2006).

4. Overview of test specimen

Experimental results were obtained for four, approximately quarter-scale, wall specimens with

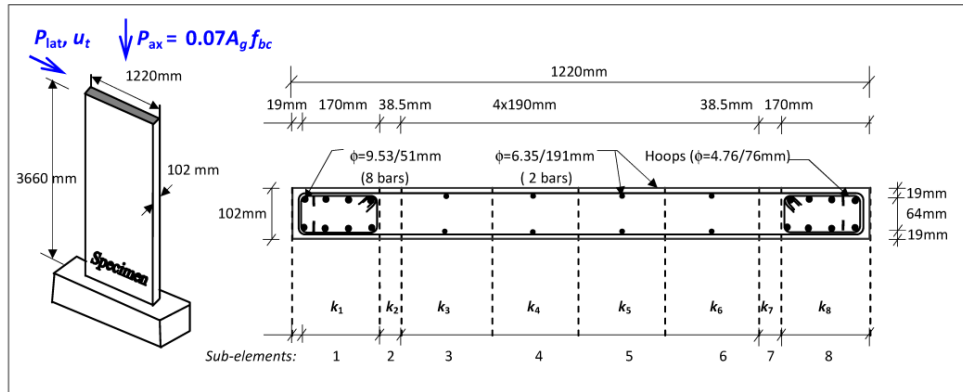


Fig. 5 Wall cross sectional views and model discretization (Thomsen and Wallace 2004)

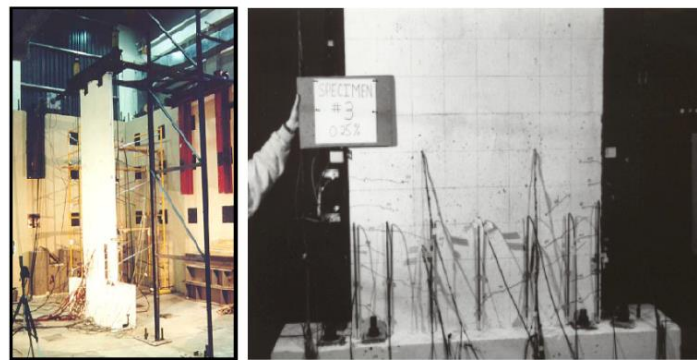


Fig. 6 Photograph of test setup and first story experimental protocol (Thomsen and Wallace 2004)

rectangular cross section, tested by Thomsen and Wallace (1995). The wall specimen was proportioned based on a prototype building designed using the strength requirements of the Uniform Building Code (UBC (1997)). A brief overview of this study is provided in the following sections, with more detailed information concerning the wall presented in Thomsen and Wallace (Thomsen and Wallace 1995, 2004).

The wall specimen was 3.66 m tall and 102 mm thick, with web length of 1.22 m. Vertical steel consisted of 8 - #3 bars ($\phi=9.53$ mm), whereas web reinforcement consisted of two curtains of deformed #2 bars ($\phi=6.35$ mm) placed horizontally and vertically, with a spacing of 190 mm on center. Reinforcing details are shown in Fig. 5.

As mentioned by Thomsen and Wallace (1995), the wall specimen was tested in an upright position. An axial load of approximately $0.07 A_g f'_c$ (where A_g corresponds to the total cross-section area) was applied at the top of the wall by hydraulic jacks mounted on top of the load transfer device. Cyclic lateral displacements were applied using a hydraulic actuator fixed to a reaction wall. Displacements, loads, and strains at critical locations were monitored. A photograph of the setup is shown in Fig. 6. More detailed information is available elsewhere (Thomsen and Wallace 1995, Orakcal *et al.* 2004).

Table 1 Mechanical properties of concrete and reinforcing steel

Material	Parameter	Material	Parameter
Concrete in compression	f'_c (MPa)	Steel	E_{0s} (GPa)
	ϵ_0		f_{yh} (MPa)
Concrete in tension	f_{cr} (MPa)	Steel	b
	ϵ_{cr}		R
	E_c (GPa)		

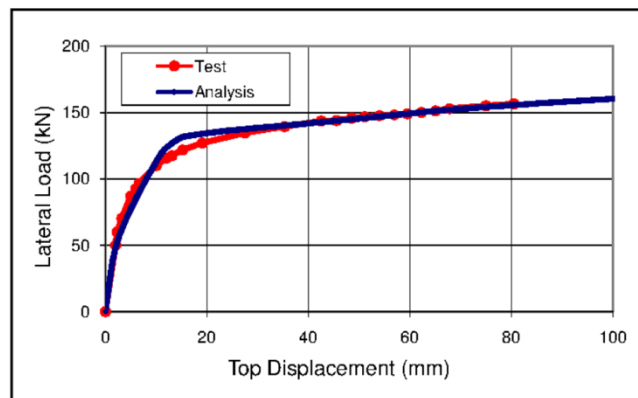


Fig. 7 Lateral load-displacement response of the specimen

5. Numerical analysis

The macro-wall-model elements formulated in §2 and the material constitutive relationships described in §3 were implemented in Matlab (Math-Works 2007) and were added to an extended nonlinear finite element (FE) structural analysis program (Hemsas 2010) together with a direct stiffness assembly procedure to assemble the macro-elements into a complete wall model (Fig. 1(b)), in order to simulate the inelastic behavior of earthquake-resistant multi-story structural walls.

A nonlinear quasi-static analysis program of the wall model was carried out using an incremental-iterative solution strategy. A displacement-controlled iterative solution strategy based on a specified incrementation of a selected displacement component (at a selected degree of freedom) was adopted in this study. Iterations were performed on both displacement and load components to obtain static equilibrium within a specified tolerance, while keeping the value of the selected displacement component constant. Details of this iterative strategy are presented by Clarke and Hancock (1990).

The wall was subjected to top displacement histories determined using the loading protocol outlined in §4. The measured axial load histories applied on the wall specimen during testing, as measured by load cells during testing, were applied to the analytical model (on average, approximately 7% of the axial load capacity for the wall specimen (see Fig. 5).

Table 1 summarizes the various parameters used in the Kent-Scott-Park (for concrete) and Menegotto-Pinto (for steel) models.

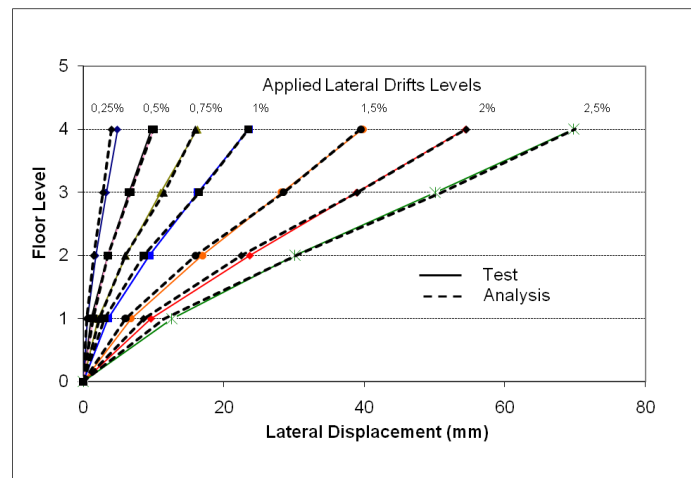


Fig. 8 Lateral displacement profiles of the wall macro-element

6. Analysis results and ability of the model to capture the wall response

Comparisons between model predictions of the flexural responses and test results are summarized in the following paragraphs.

Fig. 7 compares the envelope curve of the measured and predicted lateral load – top flexural displacement response. The analytical results were obtained using a model configuration with eight macro-elements along the height of the wall, eight uniaxial sub-elements in each macro-element, and $c=0.4$ for an applied lateral load at the top of the wall similar to the one used in the test program (cyclic drift levels of 0.1, 0.25, 0.5, 0.75, 1, 1.5, 2, and 2.5%).

Comparison with experimental results indicate that the analytical model captures reasonably well the measured response, particularly in the elastic range (initial stiffness) and in the plastic range, including stiffness degradation; therefore, the properties of the implemented analytical stress-strain relations for steel and concrete produce good correlation for global response. The lateral capacity of the wall is predicted very closely for most of the lateral drift levels. However, the model slightly overestimates the wall capacity at intermediate displacements levels (between 15 and 30 mm). This can be explained by the uncertainty in the calibration of the parameters governing the implemented steel stress-strain relation (the strain-hardening ratio b and the curvature parameter R) and by the parameters associated with concrete tensile strength (f_{cr} and ε_{cr}). A little underestimation of the stiffness is also noted for displacements levels between 7 and 15 mm. These comparisons confirm that the model provides a flexible and reliable platform for analyzing nonlinear structural walls.

Fig. 8 compares the lateral flexural displacements at various elevations of the wall, at peak top displacement (top displacement reversal) for each drift level, measured by the horizontal wire potentiometers (see Fig. 6) with the results of the analysis. The analytical macro-element model accurately captures the displacement profile.

Fig. 9 shows the normal (vertical) stress histories predicted in each sub-element (from 1 to 8) of the macro-element located at the base of the wall. The evolution of the stiffness of each sub-element is marked by three stages. A first phase elastic, with negligible loss of stiffness is considered (non-cracked concrete). A second phase post-elastic where micro-cracks of concrete

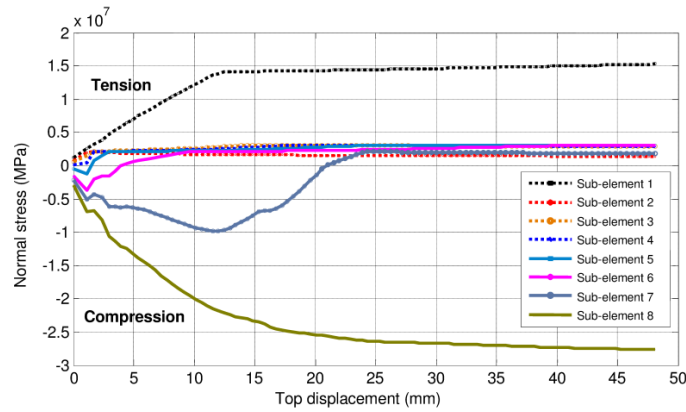


Fig. 9 Evolution of longitudinal stresses histories at the base of the wall macro-element of the eight sub-elements versus the top displacement

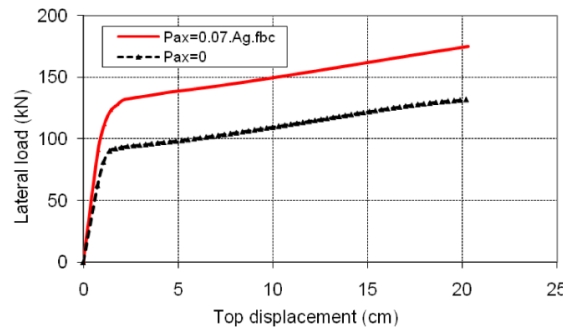


Fig. 10 Influence of axial load on the macro-model response

initiated and tends to propagate corresponding to the applied-load during its increase; the first significant cracks appear between 2.5 and 5.0 mm, resulting in a loss of stiffness which leads to failure by cracking. A final phase of stabilization can be seen with yielding of reinforcing steel bars at from 10 mm. The significant loss of rigidity of the sub-element #7 (between 5 and 25 mm) can be explained by the fact that it is devoid of any steel reinforcement and progressively crushes (see Fig. 5). It is also noted that because of progressive damage, some sub-elements (#5, #6, #7) which were initially in compression, are first damaged then become tensed while the neutral axis moves right and sub-element #8 remains in compression. Once the cracking process begins, load redistribution occurs causing the shift of the neutral axis towards the compression zone and stabilizes between sub-elements #7 and #8.

In a general sense, it may be stated that the wall macro-element model offers an attractive alternative both in the economy of computation and in the flexibility of finite element discretization based on a detailed interpretation of the local behavior (Fig. 9). This ability of a macro-model (or meso-scale model) to capture, with acceptable accuracy, the overall behavior pattern using simplified extensions from the “micro” level makes it ideal for RC modeling.

Furthermore, the model can directly consider the effect of varying axial load on the wall response, which although constant in this case, might vary in some cases (for example, under

dynamic loads such as earthquakes). Fig. 10 shows a comparison of the analytically predicted lateral load versus top displacement responses for an applied axial (vertical) load of zero and 7% of the axial load capacity of the wall, clearly displaying the significant impact of axial load on the wall response. This statement may easily be explained by the confinement of concrete.

The sensitivity of the results obtained with the model to material parameters is not addressed in this study. However, it has been done in a prior work (see (Hemsas 2010, Hemsas *et al.* 2009)). It has been observed that the predicted load-displacement response is, as expected, influenced by the properties of the stress-strain laws assumed for the longitudinal reinforcement and the concrete. Further details and discussions about these topics can be found in the above-mentioned references. Therefore the authors concluded that the use of relatively simple constitutive laws for the materials including tension stiffening provided a reliable model well-suited for practical nonlinear analysis of multistory RC structural wall systems, particularly in the context of performance-based seismic design.

We will focus hereafter on characteristic features of the model, as well as the identification of the decrease of the global stiffness (as a function of a damage variable) at various locations on the structural wall by conducting static and dynamic analyses for accurate estimation of seismic performance of the RC structural wall structures. The following section presents an overview of the applied dynamic methodology adopted in this study, through approximate Incremental Dynamic Analysis (IDA), to the two-dimensional finite macro-element modeling.

7. Simplified non-linear seismic analysis

Incremental Dynamic Analysis (IDA) is a procedure developed for accurate estimation of seismic demand and capacity of structures under seismic action. Originally proposed by Vamvatsikos and Cornell (2002), the procedure requires Non-Linear Response History Analysis (NL-RHA) of the structure for an ensemble of ground motions, each scaled to many intensity levels, selected to cover the entire range of structural response—all the way from elastic behavior to global dynamic instability. Recognizing that IDA of real structures is computationally extremely demanding, an approximate (simplified) procedure based on pushover analysis is developed (see Fig. 11). This procedure is arrived at by neglecting the coupling of the modal coordinates instead of performing complete (or “exact”) NL-RHA. Originally proposed by Chopra and Goel (2002) and adopted by the FEMA-440 guidelines (FEMA 2005), the method is a nonlinear decoupled modal analysis, denoted by Uncoupled Modal Response History Analysis (UMRHA). It is mainly characterized by modal pushover analysis according to the dominant modes of vibration of the structure. In this method, an equivalent single-degree-of-freedom (SDOF) system is defined to approximate the static pushover curve for a multi-degree-of-freedom (MDOF) structure and then determine the history response of the structure by combining the temporal responses associated with each mode of vibration. The total response of the structure is obtained by summing the contributions of the dominant modes. The decoupling of nonlinear history responses associated with each mode is the strong assumption of the UMRHA method. This assumption is deemed acceptable because although modes other than the n th-mode will participate in the solution, the n th-mode solution will be dominant. Chopra and Goel (2002) illustrate this point by performing a nonlinear time history analysis on the first three modes of the structure. This approach results in satisfactory estimations of IDA curves, provided the use of adequate models for representing the hysteretic behavior of the modal SDOF systems, in which a simple elastic-plastic model is used.

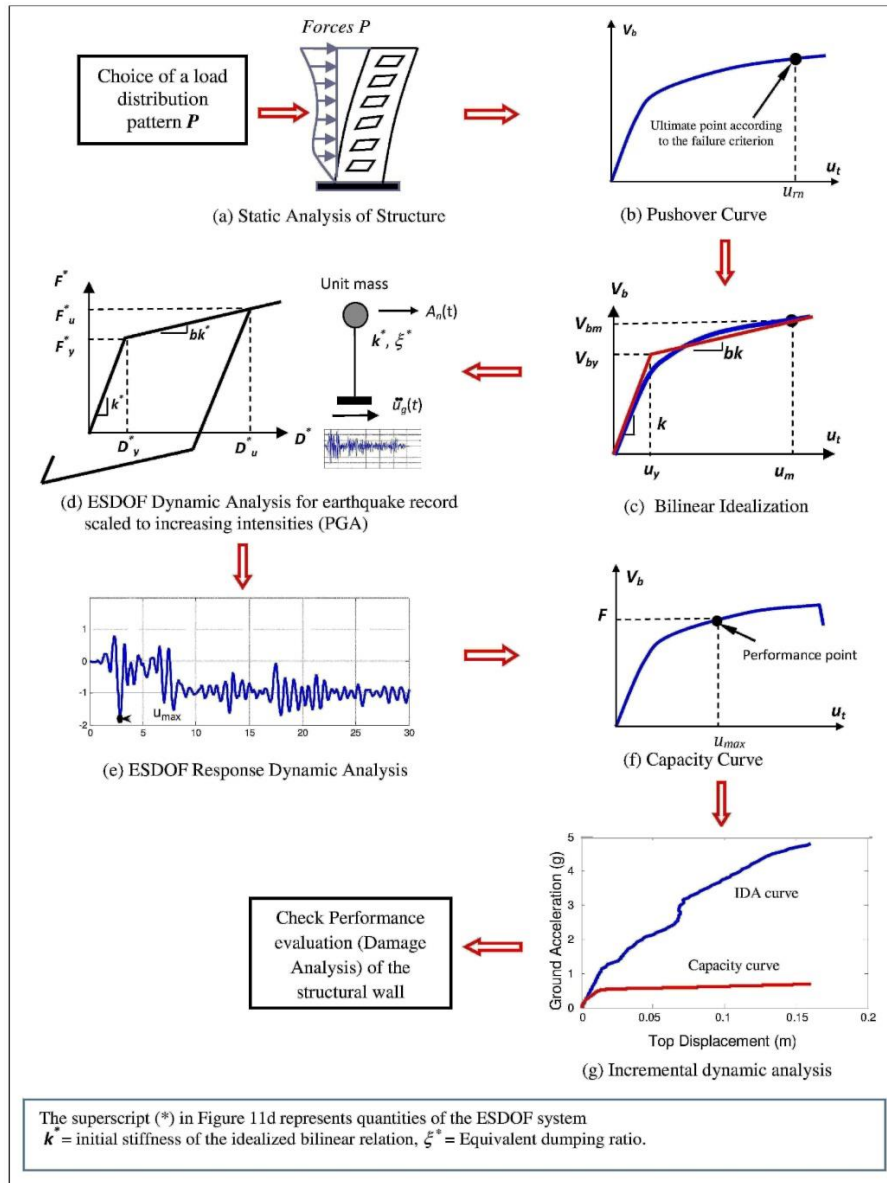


Fig. 11 Flowchart of the proposed procedure

Finally, approximate IDA is certainly particularly well-suited to simulate structural damage caused by earthquakes, involving capacity evaluation and seismic performance of RC structural wall structures. For this purpose, the identification of the global stiffness decrease as a function of a damage variable (damage index) is carried out by means of this simplified methodology.

In this section, we study qualitatively the properties and the seismic demand predictions of structural wall building, modeled by macro-elements, including capacity curves obtained with approximate IDA method, in the form of “dynamic capacity curves”. The results of these analyses

for one ground motion lead to one IDA curve. This is a plot of the ground motion intensity against a seismic demand parameter (or Damage Measure). The ground motion intensity, measured by an Intensity Measure is characterized by means of Peak Ground Acceleration (PGA), but this choice is not unique. The demand parameter may be the maximum displacement at the top of the structure (u_{\max}) or maximum inter-story drift, defined as the story drift divided by the story height.

Basic steps of the proposed method are shown in Fig. 11 and described as follows:

Step 1: Load distribution pattern and Pushover analysis

A pushover analysis is performed by subjecting a structure to a monotonically increasing pattern of lateral forces, accounting for both geometric and material non-linearities. The load distribution pattern used for pushover analysis should give an approximation of inertia force distribution during earthquakes, and make the structure vibrate in a deflection profile close to that of the fundamental mode. According to previous works, some load distribution patterns have been employed, such as the modal shape distribution of the elastic first mode from eigenvalue analysis, uniform distribution, and inverted triangular distribution for buildings, etc. (FEMA 2005). In this investigation, considering the complexity of behavior of buildings with structural walls, a Modal shape distribution of the predominant mode resulting from eigenvalue analysis, expressed as $\{F_i\}=\{m\phi_i\}$, is considered in which ϕ_i is the i th-mode of natural vibration (Fig. 11(a)). Such a distribution has a physical basis (inertia forces), and yields the simplest transformation from MDOF to SDOF systems. However, any other reasonable distribution can also be used (Fajfar 2000).

It should be noted that a failure criterion is used to determine when an ultimate state is reached during a pushover process (i.e., the ultimate point at the base shear–displacement curve, which characterizes the displacement capacity of the structure). To the knowledge of the authors, no specific proposal concerning reinforced concrete walls exists. Based on extensive test results, maximum strain criteria of steel reinforcement have been accepted as the failure criteria for a reinforced concrete element in bending. The ultimate level implies that total collapse occurs from the material strain point of view, it can be interpreted as the state whereby the longitudinal reinforcement reaches the ultimate strain ε_{su} , defined as 25 times the yield strain ε_{sy} (Hemsas 2010, Hemsas *et al.* 2010).

A representative node (control node) for monitoring deformation as well as the behavior of the wall building is defined, which is the reference displacement (here top displacement) during the pushover analysis.

By pushover analysis, the base shear versus top displacement (V_b-u_t) curve of the structure, usually called capacity curve, is obtained. The ultimate state point at the V_b-u_t curve is found according to the failure criterion, (Fig. 11(b)).

Step 2: Bilinear idealization

The original V_b-u_t curve is then idealized to a bilinear relationship, which defines the yield strength V_{by} , the yield displacement u_y , the effective stiffness k and the hardening stiffness bk (Fig. 11c). The idealization method based on the energy conservation criterion is applied so as to make the absorbed energy of the idealized curve equal to that of the original pushover curve.

Step 3: Transformation of the established MDOF system to equivalent SDOF model

According to previous work based on non-linear pushover analysis (Fajfar 2000, Chopra and Goel 2002) the established MDOF system (capacity curve) is transformed into an equivalent

SDOF model (Fig. 11(d)), which is used later to determine the seismic demand. For this purpose, there are some optional methods, such as inelastic spectra, elastic spectra or direct time-history analyses of the equivalent SDOF system with selected accelerogram input (Chopra 2007). The last method is adopted in this study.

Step 4: Displacement demand of the original MDOF model

The maximum displacement u_{\max} of the equivalent SDOF system under the specified earthquake ground motion is obtained (Fig. 11(e)) and transformed to the corresponding displacement demand of the original MDOF model (Fig. 11(f)). Then the performance at the expected maximum displacement is evaluated on the global and local level. It should be noted that the maximum top displacement u_t of the MDOF system (the reference displacement) is obtained by multiplying the displacement demand for the equivalent SDOF model with the transformation factor, usually called the modal participation factor.

Note that seismic demands for all relevant local quantities are obtained by assuming that the distribution of deformations throughout the structure in the static (pushover) analysis approximately corresponds to that which would be obtained in the dynamic analysis (Fajfar 2000).

Step 5: Approximate IDA analysis

To perform incremental dynamic analysis (IDA), a single record representing a scenario earthquake is used. This record is appropriately scaled to increasing intensities designed to force the structure all the way from the onset of damage to final global dynamic instability or collapse (Fig. 11(g)). Thus, we can generate IDA curve of the structural response (MDOF system), as measured by a Damage Measure (DM , e.g., top displacement or maximum inter-story drift), versus the ground Motion Intensity level, measured by an Intensity Measure (IM , e.g., peak ground acceleration). Because of the “load-incrementing” nature of this more recent procedure one can track the structural performance across all response levels and limit-states and extract useful information about the accuracy and stability of structural members (in our study, structural wall) under both static and dynamic loads.

Step 6: Performance evaluation (Damage Analysis):

An important issue in Performance-Based Earthquake Engineering is the estimation of structural Performance under seismic loading, signifying that collapse does not occur under selected ground motions (i.e., the structure maintains stability, and deformations are within acceptable limits). IDA curve established in the previous step contains the necessary information to assess this issue. Subsequently, the state of damage in the structure is induced by subjecting the structural model to multiple levels of seismic intensity of the selected ground motion record and the stiffness degradation of the building due to seismic excitation is directly linked to the global structural damage (damage index) varying between 0 (no damage) and 1 (global collapse), as it will be described later in § 9. It could be noted that global collapse is related to the IM or DM value where dynamic instability is observed.

In general, it is presumed that the onset of structural damage will typically occur at forces and deformations beyond the yield point, with some permanent deformation associated with cracking of concrete and yielding of steel. For reinforced concrete components, the onset of damage is likely to involve slight spalling, slight yielding of longitudinal reinforcement, and cracking of concrete with residual crack widths (Brown and Lowes 2007).

This proposed procedure based on Uncoupled Modal Response History Analysis (UMRHA) of

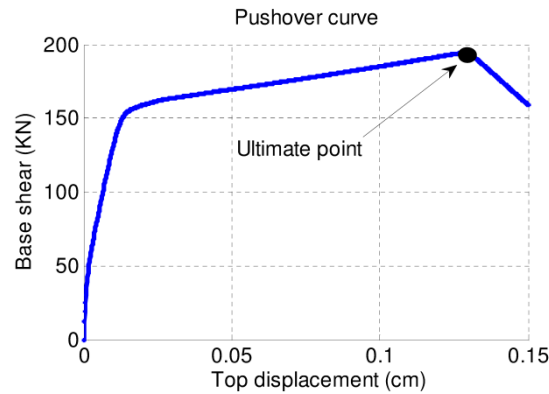


Fig. 12 Load–displacement curve corresponding to the first mode distribution loading

an equivalent SDOF system approximation can give close estimation results for seismic capacity and demand predictions of the structure, involving both displacement capacity determination and simplest verification method which can be processed and summarized to get the distribution of representative damage measure (DM) given intensity IM .

8. Case study and results

The same idealized building with structural wall examined in § 5 and macro-elements model (Fig. 5) were used for investigation of the procedure. A prototype building, representing a typical multistory office building in an area of high seismicity (Los Angeles), was used to assist in determining the wall geometry and reinforcing details for the testing program. Experimental verification of the proposed displacement-based design approach by Wallace (1994, 1995) involved the testing of six, approximately quarter-scale, wall specimens. The walls tested included rectangular and T-shaped structural walls and moment-resisting frames to resist lateral loads. Results for the walls with T-shaped are presented elsewhere (Wallace (1994, 1995)). Additional details of the analyses and the resulting prototype walls are reported by Thomsen and Wallace (1995); therefore, only results for the rectangular walls cross sections are presented.

For pushover analysis, the force pattern corresponded to the product of the story masses and the most important mode shape (in our case the first mode) is applied, as recommended by EC8 (CEN, 2005). In Fig. 12 the so-called collapse limit state point (corresponding to the ultimate displacement) is also shown in the post-capping part of the pushover curve. Theoretically, predicted top displacement at collapse is approximately 16 cm. The failure was observed at a base shear value of approximately 206 kN.

The equivalent ESDOF model was then defined and the dynamic IDA-capacity curves were computed by using the direct nonlinear Uncoupled Modal Response History Analysis (UMRHA). The accelerogram used in the IDA analysis is generated from the real accelerogram recorded during the 1940 Elcentro Earthquake N-S component (Fig. 13).

This record was appropriately scaled to cover the entire range of structural response, from elasticity, to yielding, and finally global dynamic instability. At each scaling level a nonlinear dynamic analysis was performed and the Engineering Demand Parameters (EDPs) were extracted.

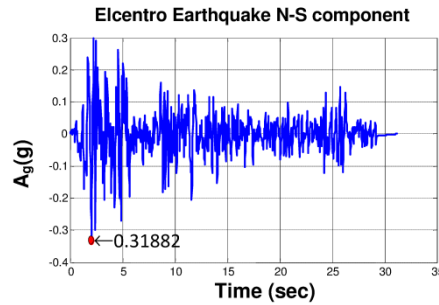


Fig. 13 Ground Acceleration of N-S Component of Elcentro Earthquake (in g)

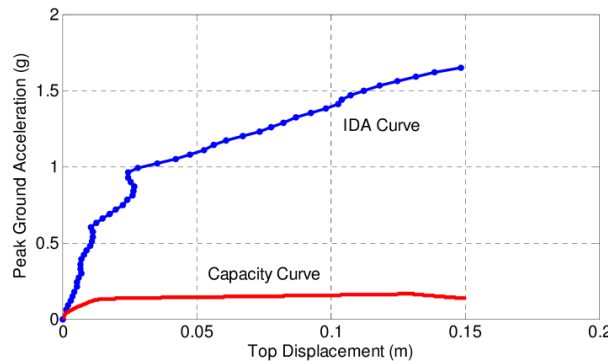


Fig. 14 IDA curve and capacity diagram presented for peak ground acceleration versus maximum top displacement

By interpolating such pairs of *IM* and EDP values for the individual record we get a continuous IDA curve, presented in terms of peak ground acceleration (*PGA*) versus top displacement, as shown in Fig. 14. The peak ground acceleration, which causes the ultimate dynamic instability of the structure, is about 1.6g. This is rather high value because of heavily reinforced structural wall. However, structure starts degrading if peak ground acceleration is about 0.1g (see Fig. 15). This can be concluded if capacity diagram (for the MDOF model) is compared with the IDA curve (Fig. 14). More details regarding the evolution of damage on the structural wall with the peak ground acceleration is presented in the following section.

9. Identification of damage levels

In the seismic design of structures, the concepts of damage and damageability play a central role. It is accepted that standard design procedures, based on the concept of the force reduction factor, even if adequate in most practical cases, do not result in structures with uniform and rationally defined safety and performance levels. For this reason, the concept of damage indices or damage indicators has become popular. In general, damage indicator (or damage index *DI*) is usually related to deterioration of structural resistance. The damage indicator can be used for seismic evaluation of structures with given properties and can provide information of potential damage of the recorded ground motions.

Table 1 Parameters defining the input motion of run

Runs	PGA (g)
Run-1	0.05
Run-2	0.1
Run-3	0.5
Run-4	1.0
Run-5	1.5

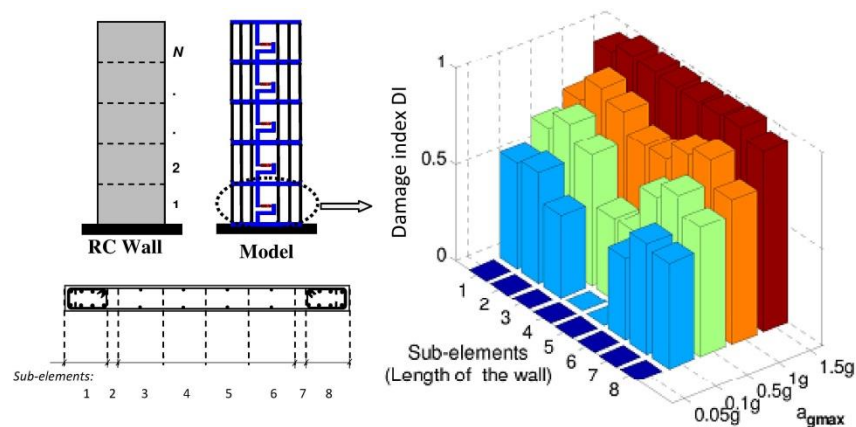


Fig. 15 Level of degradation (DI) of structural-wall sub-elements at the bottom (First storey)

Therefore many damage models have been developed (Krawinkler and Nassar 1992, Powell and Allhabadi 1988). These models are the product of a broad knowledge and expertise of behavior of structures under seismic loading, resulting as well from the observation of actual earthquakes as of laboratory experiments. To the knowledge of the authors, no specific proposal concerning reinforced concrete walls has been developed. The simplest global Damage Index, inspired of the proposition of Powell and Allahabadi (1988), is defined as

$$DI = 1 - \frac{K_{current}}{K_{initial}} \quad (16)$$

This damage index which is evaluated based on the stiffness degradation of all sub-elements, varies according to the deformation level of the wall macro-element at basic level cross section. It is normalized so that its value is equal to zero when there is no damage (i.e., linear elastic behavior of the structure during earthquake), and is equal to unity when total collapse or failure occurs (i.e., local or global collapse of the structure).

9.1 Collapse process of structural-wall elements

The onset of significant component degradation is also an important indicator to evaluate the accuracy of the analysis and the extent to which the model can accurately capture the strength and stiffness degradation that occurs at larger deformations.

The degree of stiffness degradation and strength deterioration expressed in terms of damage

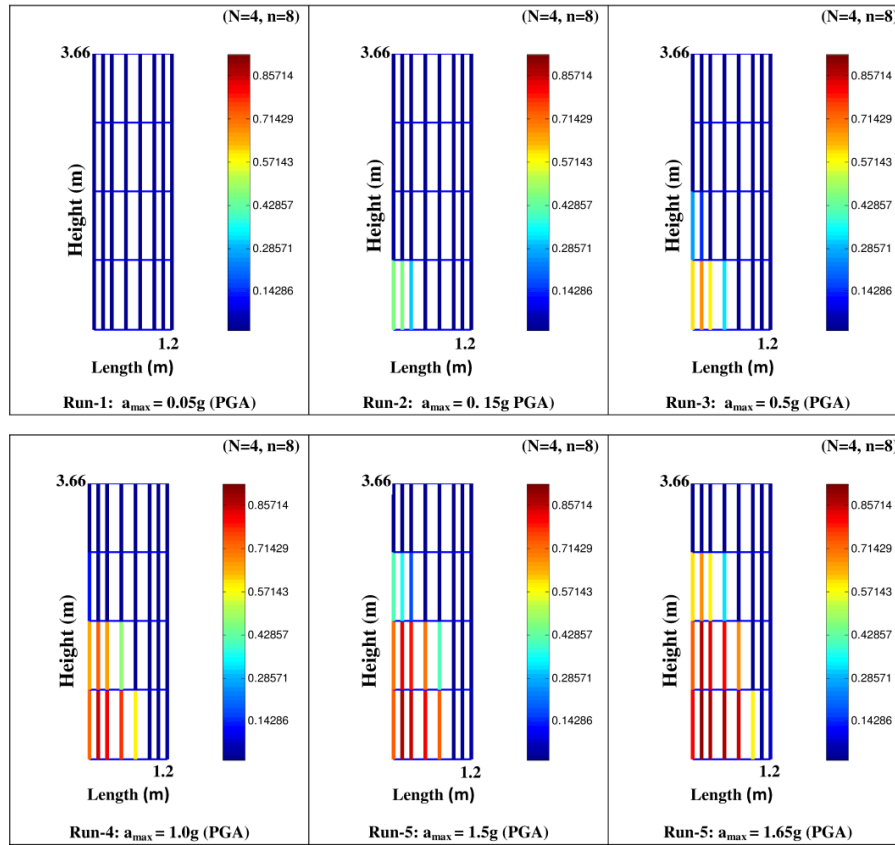


Fig. 16 Collapse process of structural-wall macro-elements

index (*DI*) of the macro-element wall model is shown in Fig. 15. The results are plotted for all sub-elements (*n*) in the wall at basic level cross section, and various $a_{g,max}$ (*PGA*). The study was conducted after scaling the input motions of Elcentro Earthquake record to five selected levels of peak ground acceleration (*PGA*) values (as illustrated in Table 2).

A close examination of Fig. 15 reveals that potential damage of the structural wall starts at input motion of *Run-2* (0.1g). *Run-4* (1g) caused substantially higher stiffness degradation. On the other hand, heavy damage of the wall occurred at the end of *Run-5* (1.5g). Other stories are also damaged as shown in Fig. 16. The whole structural wall fail at last due to the decrease of the resistance capacity of lateral load after most concrete is crushed and steel bars are yielded.

9.2 Comparison of local collapse status of specimen

The simulation of collapse process of structural wall macro-elements can be improved by an in-depth analysis of the nonlinear degradation states of sub-elements under different levels of peak ground acceleration. Take for example *Run-3*, as shown in Fig. 17(a), plastic deformation (failure mechanism) mainly occurs at the bottom. Energy can be dissipated through prejudicial cracking of the concrete and yielding of the reinforcing bars. The concrete of both sides is subsequently crushed and out of work. The crushed concrete extends from edge to center part. If no

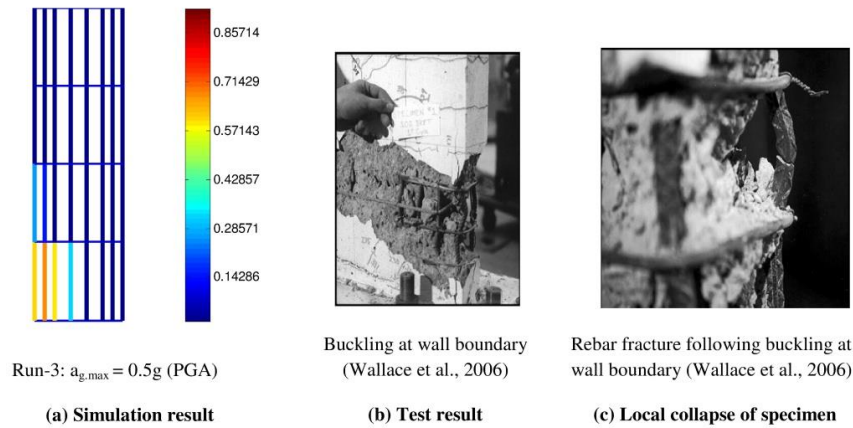


Fig. 17 Comparison of local collapse status of specimen

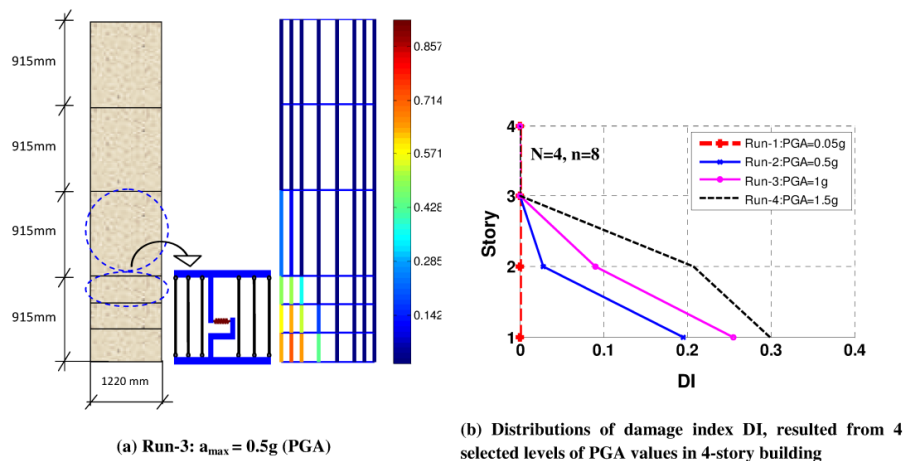


Fig. 18 Sensitivity of the model discretization of the four-storey wall and structural damage indices resulted from the four selected levels of PGA values

reinforcement is provided (as in the case of sub-elements #2 and #7 in our macro-element model), sudden failure will be expected when the first crack occurs. Towards the top of the wall, there is a decrease in the degradation corresponding to lower values of the damage index between 0.15 and 0.35, representing a slight degradation due to less cracking in these areas.

The failure mode comparison of the specimen with test results conducted by Wallace *et al.* (2006) is shown in Fig. 17. Instabilities, such as rebar buckling and lateral web buckling, and rebar fracture were typically observed (Fig. 17(b)). The damage to the free edge of the rectangular specimen wall after the final test is also illustrated. Clearly, this wall would not survive (very strong) loading without substantial amount of confining reinforcement. Ductility can be obtained by placing confined reinforcement in areas positioned at the edges of the cross section, often called “edge elements”. In such areas the first set of concrete spalling will occur, and consequently we can prevent the damage by strengthening these areas.

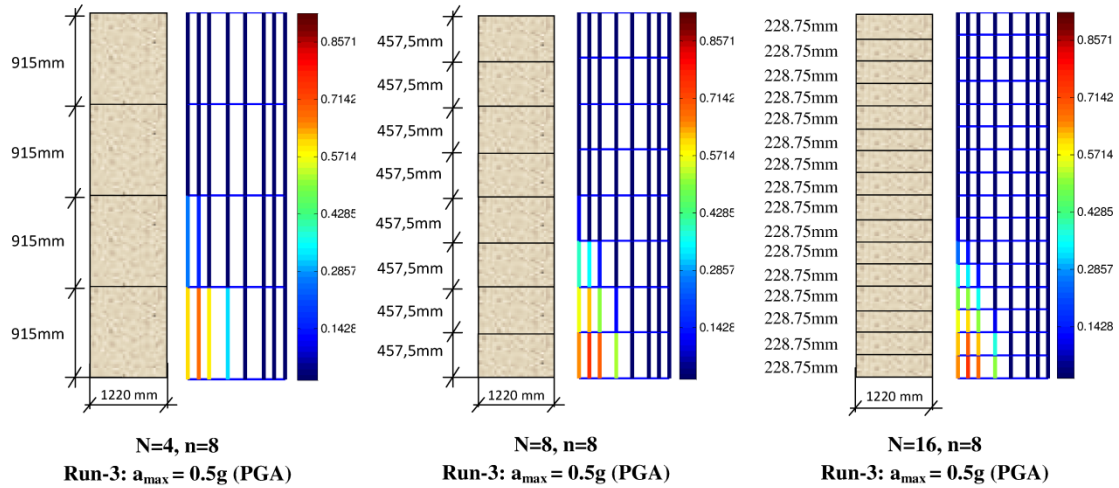


Fig. 19 Global degradation map of the wall using 4, 8 and 16-structural wall macro-elements

In order to demonstrate the effectiveness and ability of the macro-element model in predicting the nonlinear dynamic response and verify the sensitivity of the predicted wall responses to changes in model discretization (especially the number of macro-elements N), a refined model is used (Fig. 18(a)). In this model one macro-element is used for each story except for the first story, where the flexural plastic hinge will be located. This story is discretized into three macro-elements.

Fig. 18(b) indicates the structural damage indices resulting from the four selected levels of peak ground acceleration (PGA) values, using a model with one macro-element for each story building. It can be seen that DI overall is less than 0.3, which means that building does not undergo severe damage. This damage does not show the distribution value of relative drift, hysteretic energy and structural damage in stories.

Finally Fig. 19 compares the global degradation map of the wall using a structural wall model of 4, 8 and 16-structural wall macro-elements, each with 8 sub-elements. It seems that by increasing the number of macro-elements, height-wise distribution of damage in the three models is almost similar. Based on numerical simulation results, it was verified that location of major cracks and failure mechanism predicted by the macro-element model reasonably matches with the experimental observations in a way that in each model, collapse process occurs at the base of the rectangular structural wall, which fits well with the philosophy of EC8 (CEN 2005) which foresees the development of a plastic hinge (See Fig. 17). It can also be seen that the three models have a very similar degradation, confirming that the discretization does not have a significant affect either on the overall response of the wall or the damage facies. Its simplicity, the model can adequately describe the overall behavior of the structure. Moreover, it is able to qualitatively reproduce the trends of global degradation of rigidity and the position of damage areas.

5. Conclusions

The intent of this paper was to investigate seismic response and damage detection analyses of

an RC structural wall building using reliable and robust macro-element model that incorporate relatively simple constitutive material laws and demonstrate the effectiveness of this model for simulating the inelastic response of reinforced concrete structural walls.

The analytical model was subjected to the same loading protocol with that experienced during testing by Thomsen and Wallace. The correlation of the experimental and analytical results was investigated in detail, at various response levels and locations (story displacements, average strains over the first story level). It was observed that the macro-element model, as implemented here, provides a good prediction of flexural responses (lateral load capacity and lateral displacement profile at varying drift levels) of the wall. The analytical model is also able to simulate important behavioral features of the experimentally observed behavior including shifting of the neutral axis along the wall cross section, which is commonly ignored in simple models. Characteristics of the global response, including stiffness degradation, are clearly captured.

A simplified methodology for the evaluation of seismic performance of earthquake resistant structures with structural walls was next carried out, based on capacity method and approximate Incremental Dynamic Analysis of an equivalent SDOF system using a damage index. This parameter which can be used also for seismic evaluation of vulnerability of structures with given properties provides useful information of potential damage of the recorded ground motion parameters with respect to stiffness deterioration of the structural wall.

In the light of above findings, there is no doubt that approximate IDA analysis of equivalent SDOF system provides a very thorough image of the seismic behavior of the structural wall building, even though of fewer DOFs. The location of major crack and overall cracking pattern predicted by IDA method reasonably matches with the experimental observations at meso-scale. The proposed methodology can be adopted with reasonable confidence in seismic qualification as well as reassessment of structures.

Overall, the use of macro-element model provides an effective means for modeling the flexural response prediction of reinforced concrete structural walls at both global and local levels. Implementation of the model into a computational program will provide design engineers improved analytical capabilities to model the behavior of structural walls.

Future work will focus on modeling of walls with different reinforcement and various cross sections, modeling of the shear response, as well as developing, in a follow-up paper, a procedure to integrate wall openings.

References

- Bakir, P.G. and Boduroglu, H.M. (2006), "Nonlinear analysis of beam-column joints using softened truss model", *Mech. Res. Commun.*, **33**(2), 134-147.
- Belarbi, H. and Hsu, T.C.C. (1994), "Constitutive laws of concrete in tension and reinforcing bars stiffened by Concrete", *ACI Struct. J.*, **91**(4), 465-474.
- Belmouden, Y. and Lestuzzi, P. (2007), "Analytical model for predicting nonlinear reversed cyclic behaviour of reinforced concrete structural walls", *Eng. Struct. J.*, **29**(7), 1263-1276.
- Brown, P.C. and Lowes, L.N. (2007), "Fragility functions for modern reinforced-concrete beam-column joints", *Earthq. Spectra*, **23**(2), 263-289.
- CEN (2005), *Eurocode 8: Design of Structures for Earthquake Resistance. Part 3: Assessment and Retrofitting of Buildings, Stage 64*, European Committee for Standardisation, Brussels, March.
- Chopra, A.K. and Goel, R.K. (2002), "A modal pushover analysis procedure for estimating seismic demands for buildings", *Earthq. Eng. Struct. Dyn.*, **31**(3), 561-582.

- Chopra, A.K. (2007), *Dynamics of Structures: Theory and Applications to Earthquake Engineering*, 3rd edition, Pearson Prentice-Hall, Upper Saddle River, New Jersey, USA.
- Clarke, M. J. and Hancock, G.J. (1990), "A study of incremental-iterative strategies for non-linear analyses", *Int. J. Numer. Method. Eng.*, **29**(7), 1365-1391.
- Elmorsi, M., Kianush, M.R. and Tso, W.K. (1998), "Nonlinear Analysis of Cyclically Loaded Reinforced Concrete Structures", *ACI Struct. J.*, **95**(6), 725-739.
- Fajfar, P. (2000), "A nonlinear analysis method for performance-based seismic design", *Earthq. Spectra*, **16**(3), 573-592.
- Fajfar, P. and Fischinger, M. (1988), "N2-a method for non-linear seismic analysis of rectangular buildings", *Proceedings of the 9th World Conference on Earthquake Engineering*, Tokyo-Kyoto, Japan.
- FEMA-440 (2005), *Improvement of Nonlinear Static Seismic Analysis Procedures*, DC: Federal Emergency Management Agency, Washington, USA.
- Filippou, F.C., D'Ambrisi, A. and Issa, A. (1992), *Nonlinear Static and Dynamic Analysis of Reinforced Concrete Subassemblages*, Report No. UCB/EERC-92/08, Earthquake Engineering Research Center, University of California, Berkeley, California.
- Fischinger, M., Vidic, T. and Fajfar, P. (1991), "Evaluation of the inelastic response of a RC building with a structural wall designed according to Eurocode 8", *Proceedings, International Conference on Buildings with Load Bearing Concrete Walls in Seismic Zones*, Paris, France.
- Fischinger, M., Vidic, T. and Fajfar, P. (1992), "Nonlinear Seismic Analysis of Structural Walls Using the Multiple-Vertical-Line-Element Model", *Nonlinear Seismic Analysis of RC Buildings*, Eds. Krawinkler, H. and Fajfar, P., Elsevier Science Publishers Ltd, London and New York.
- Hemsas, M. (2010), "Modélisation par macro-éléments du comportement non-linéaire des ouvrages à voiles porteurs en béton armé sous action sismique (Développement de méthodes simplifiées d'analyse dynamique et de vulnérabilité sismique)", Thèse de doctorat, Université de Bordeaux, France.
- Hemsas, M., Elachachi, S.M. and Breysse, D. (2009), "Modélisation par macro-éléments du comportement non-linéaire des murs voiles en béton armé", *Eur. J. Environ. Civil Eng.*, **13**(5), 615-640.
- Hemsas, M., Elachachi, S.M. and Breysse, D. (2010), "Evaluation of the seismic vulnerability of quasi symmetrical reinforced concrete structures with shear walls", *Eur. J. Environ. Civil Eng.*, **14**(5), 617-636.
- Hsu, T.T.C. and Zhu, R.R.H. (2002), "Softened membrane model for reinforced concrete elements in shear", *ACI Struct. J.*, **99**(4), 460-469.
- Kabeyasawa, T., Shiohara, H., Otani, S. and Aoyama, H. (1983), "Analysis of the full-scale seven-story reinforced concrete test structure", *J. Facult. Eng., Univ. Tokyo (B)*, Tokyo, Japan, **37**(2), 431-478.
- Kent, D.C. and Park, R. (1971), "Flexural members with confined concrete", *ASCE J. Struct. Div.*, **97**(7), 1969-1990.
- Scott, B.D., Park, R. and Priestley, M.J.N. (1982), "Stress-strain behavior of concrete confined by overlapping hoops at low and high strain rates", *J. Am. Concrete Ins.*, **79**(1), 13-27.
- Krawinkler, H. and Nassar, A.A. (1992), "Seismic design based on ductility and cumulative damage demands and capacities", Eds. Fajfar, P. and Krawinkler, H., *Nonlinear seismic analysis and design of reinforced concrete buildings*, Elsevier Applied Science, New York.
- Lestuzzi, P. and Bachmann, H. (2007), "Displacement ductility and energy assessment from shaking table tests on RC structural walls", *Eng. Struct.*, **29**(8), 1708-1721.
- Mander, J.B., Priestley, M.J.N. and Park, R. (1988), "Theoretical stress-strain model for confined concrete", *ASCE J. Struct. Eng.*, **114**(8), 1804-1826.
- Mansour, M., Lee, J. and Hsu, T.T.C. (2001), "Cyclic stress-strain curves of concrete and steel bars in membrane elements", *ASCE J. Struct. Eng.*, **127**(12), 1402-1411.
- Math-Works Inc. (2007), "Matlab", Inc. Natick, Massachusetts.
- Menegotto, M. and Pinto, E. (1973), "Method of analysis for cyclically loaded reinforced concrete plane frames including changes in geometry and non-elastic behavior of elements under combined normal force and bending". *Proceedings of the IABSE Symposium on Resistance and Ultimate Deformability of Structures Acted on by Well-Defined Repeated Loads*, Lisbon, Portugal.
- Miao, Z.W., Lu, X.Z., Jiang, J.J. and Ye, L.P. (2006), "Nonlinear FE model for RC shear walls based on

- multi-layer shell element and microplane constitutive model”, *Comput. Method. Eng. Sci. EPMESC X*, Sanya, Hainan, China, August.
- Orakcal, K., Wallace, J.W. and Conte, J.P. (2004), “Flexural modeling of reinforced concrete walls-model attributes”, *ACI Struct. J.*, **101**(5), 688-699.
- Pang, X.D. and Hsu T.T.C. (1995), “Behavior of reinforced concrete membrane elements in shear”, *ACI Struct. J.*, **92**(6), 665-679.
- Paulay, T. and Priestley, M.J.N. (1992), *Seismic Design of Reinforced Concrete and Masonry Buildings*, John Wiley & Sons, New York, USA.
- Powell, G.H. and Allhabadi, N. (1988), “Seismic damage prediction by deterministic methods: concepts and procedures”, *Earthq. Eng. Dyn. Struct.*, **16**(5), 719-734.
- Scott, B.D., Park, R. and Priestley, M.J.N. (1982), “Stress-strain behavior of concrete confined by overlapping hoops at low and high strain rates”, *J. Am. Concrete Inst.*, **79**(1), 13-27.
- Thomsen, J.H. and Wallace, J.W. (1995), *Displacement-Based Design of RC Structural Walls: An Experimental Investigation of Walls with Rectangular and T-Shaped Cross-Sections*, Report No. CU/CEE-95/06, Department of Civil Engineering, Clarkson University, Postdam, N.Y.
- Thomsen, J.H. and Wallace, J.W. (2004), “Experimental verification of displacement-based design procedures for slender reinforced concrete structural walls”, *ASCE J. Struct. Eng.*, **130**(4), 618-630.
- UBC (1997), *Uniform Building Code*, International Conference of Building Officials, Whittier, California, USA.
- Vamvatsikos, D. and Cornell C.A. (2002), “Incremental dynamic analysis”, *Earthq. Eng. Struct. Dyn.*, **31**(3), 491-514.
- Vamvatsikos, D. and Fragiadakis, M. (2010), “Incremental dynamic analysis for estimating seismic performance sensitivity and uncertainty”, *Earthq. Eng. Struct. Dyn.*, **39**(2), 141-163.
- Vulcano, A., Bertero, V.V. and Colotti, V. (1988), “Analytical modeling of RC structural walls”, *Proceedings of the 9th World Conference on Earthquake Engineering*, Tokyo-Kyoto, Japan.
- Vulcano, A. and Bertero, V.V. (1987), *Analytical Models for Predicting the Lateral Response of RC Shear Walls: Evaluation of Their Reliability*, EERC, Report No.UCB/EERC-87/19, Earthquake Engineering Research Center, University of California, Berkeley, California.
- Wallace, J.W. (1994), “A new methodology for seismic design of reinforced concrete shear walls”, *ASCE J. Struct. Eng.*, **120**(3), 863-884.
- Wallace, J.W. (1995), “Seismic design of reinforced concrete shear walls, Part I: New Code Format”, *ASCE J. Struct. Eng.*, **121**(1), 75-87.
- Wallace, J.W., Massone, L. and Orakcal, K. (2006), “Seismic performance of existing concrete buildings”, *100th Anniversary Earthquake Conference Press Conference, Managing Risk In Earthquake Country*, Moscone Center, San Francisco, April.